A Burst Chasing X-ray Polarimeter

Joanne E. Hill[*a,b], Scott Barthelmy[c], J. Kevin Black[c,d], Philip Deines-Jones[c], Keith Jahoda[c], Takanori Sakamoto[c], Philip Kaaret[e], Mark L. McConnell[f], Peter F. Bloser[f], John R. Macri[f], Jason S. Legere[f], James M. Ryan[f], Billy R. Smith Jr.[g], Bing Zhang[h]

[a]Universities Space Research Association, 10211 Wincopin Circle, Suite 500, Columbia, MD 21044, USA, [b]CRESST and NASA Goddard Space Flight Center, Greenbelt, MD 20771 USA, [c]NASA Goddard Space Flight Center, Greenbelt, MD 20771 USA, [d]Rock Creek Scientific, 1400 East-West Hwy, Suite 807, Silver Spring, MD 20910 USA [e]Department of Physics and Astronomy, University of Iowa, Iowa City, IA 52242 USA, [f]Space Science Center, University of New Hampshire, Durham, NH 03824 USA, [g]Department of Aerospace Engineering, United States Naval Academy, 590 Holloway Road, Annapolis, MD 21402 USA, [h]Department of Physics, University of Nevada, Box 454002, Las Vegas, NV 89154, USA

ABSTRACT

Gamma-ray bursts are one of the most powerful explosions in the universe and have been detected out to distances of almost 13 billion light years. The exact origin of these energetic explosions is still unknown but the resulting huge release of energy is thought to create a highly relativistic jet of material and a power-law distribution of electrons. There are several theories describing the origin of the prompt GRB emission that currently cannot be distinguished. Measurements of the linear polarization would provide unique and important constraints on the mechanisms thought to drive these powerful explosions.

We present the design of a sensitive, and extremely versatile gamma-ray burst polarimeter. The instrument is a photoelectric polarimeter based on a time-projection chamber. The photoelectric time-projection technique combines high sensitivity with broad band-pass and is potentially the most powerful method between 2 and 100 keV where the photoelectric effect is the dominant interaction process. We present measurements of polarized and unpolarized X-rays obtained with a prototype detector and describe the two mission concepts; the Gamma-Ray Burst Polarimeter (GRBP) for the U.S. Naval Academy satellite MidSTAR-2, and the Low Energy Polarimeter (LEP) onboard POET, a broadband polarimetry concept for a small explorer mission.

Keywords: Gamma-ray Bursts, X-rays, Gamma-rays, Polarization

1. INTRODUCTION

1.1 Scientific Motivation

Gamma-ray bursts (GRBs) are short and extremely bright bursts of gamma-rays and X-rays, detected out to cosmological distances at the rate of about 2 per week by NASA's *Swift* mission. The exact origin of these energetic explosions is still unknown but the most favored model for the prompt emission from long bursts (duration > 2 seconds) is the gravitational collapse of a massive star to form a black hole[28]. There is evidence that short GRBs (duration <2 seconds) arise from a different process and are produced from the merger of two compact objects[10,11]. The resulting huge release of energy is thought to create a highly relativistic jet of material and a power-law distribution of electrons[29]. There are several theories describing the prompt GRB emission, and which predict vastly different degrees of linear polarization (P):

- P>~80% is generally difficult to achieve within synchrotron emission models but could be achieved for an inverse Compton scattering jet viewed just outside the edge of the jet[8,16].
- 20%<P<60% is predicted if synchrotron emission is the dominant source of radiation or as a result of viewing the burst from near the edge of the jet[12,13,19].

* jhill@milkyway.gsfc.nasa.gov; phone 1 301 286-0572; fax 1 301 286-1684

- Low degrees of polarization can be expected from hydrodynamic models in which random magnetic fields are generated in the shocks with an on-beam viewing geometry.

There is evidence that the prompt gamma-ray flux from GRBs is highly polarized. The report of a high degree of polarization (~80%) in the prompt gamma-ray emission from GRB 021206[6,30,35] remains controversial due to the difficulties in modeling the instrument response to unpolarised X-rays. In an effort to constrain GRB prompt emission models, Willis et al.[36] derived polarization limits using the BATSE Albedo Polarimetry System which showed evidence of P>35% and P>50% for GRB 930131 and GRB 960924, respectively. However, only two bursts out of a catalog of more than 2600 had the required characteristics for the analysis. More recently, tentative polarization measurements have been obtained from the spectrometer onboard INTEGRAL for GRB 041219a; around 60% over several energy ranges and time intervals but at a low level of significance (~2σ)[23] and as high as 98%±33% although instrumental systematic effects could not be ruled out[15]. An instrument designed to make measurements of the polarization of the prompt GRB emission would provide a qualitative and quantitative leap forward in our understanding of the mechanisms driving GRB explosions.

1.2 Photoelectric Polarimetry

The photoelectric effect is theoretically the most sensitive technique available for broadband X-ray polarimetry below ~100 keV. Not only is it the dominant interaction mechanism in most materials, but it is also a powerful polarization analyzer. As a result of the photoionization of an atomic s-orbital, the photoelectron is ejected preferentially with a probability distribution dependent on the polarization of the incident X-ray. The angular distribution is modulated as $\cos^2\phi$, where ϕ is the azimuthal angle measured from the X-ray electric-field vector. The amplitude and phase of the modulation provides a measure of the magnitude and direction of the linear polarization of the X-ray. The magnitude and orientation of the source polarization can be determined from a histogram of the emission angles.

1.3 Time-Projection Chamber (TPC) Polarimeters

Photoelectric polarimetry has recently become more practical for astronomical applications with the development of pixelized micropattern gas detectors[1,2,3,7], see Figure 1.1, left. A micropattern proportional counter, consisting of a drift electrode and a high-field multiplication region, is suspended above a pixelized readout plane. The multiplication region shown below is gas electron multiplier (GEM)[33].

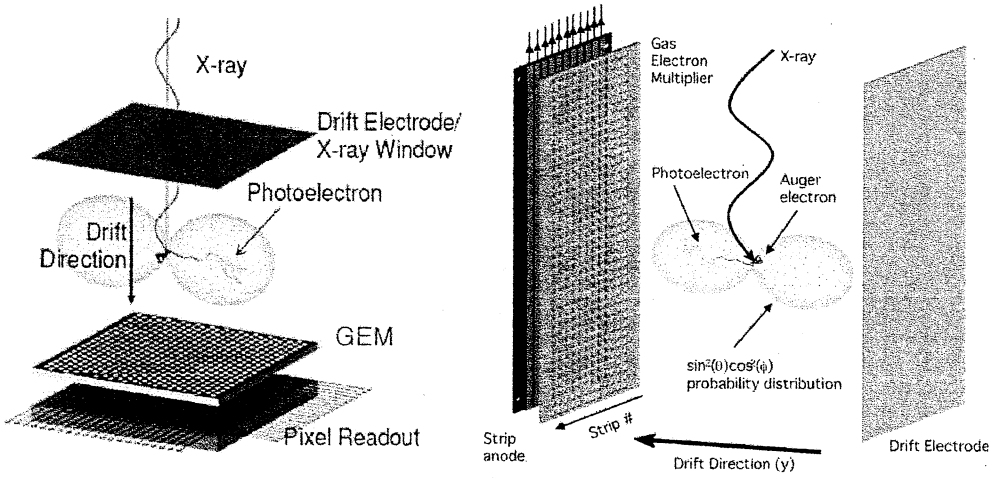

Figure 1.1 Left: A pixel polarimeter consisting of a micropattern proportional counter mounted above a pixelized detector (Courtesy J. Swank). Right: A TPC polarimeter showing the alternate geometry. The drift field is orthogonal to the direction of incident X-rays. A drift electrode is shown on the right and the multiplication stage (anode and cathode) on the left with a strip detector behind.

When an X-ray is absorbed in the gas between the drift electrode and the multiplication region, a photoelectron is ejected. As the photoelectron travels through the gas it creates a path of ionization that drifts in a moderate, uniform field to the high-field multiplication region where an avalanche occurs. The charge finally drifts to the pixel detector where it is read out. The pixels are smaller than the mean free path of the photoelectron and therefore an image of the track can be reconstructed and the initial direction of the photoelectron determined.

Despite the impressive modulations of these polarimeters, the quantum efficiency associated with peak sensitivity is rarely as great as 10% for the gas mixtures demonstrated[2]. The sensitivity is limited by the diffusion of the primary ionization electrons as they drift toward the readout plane (Figure 1.1, left). Increasing the detector depth to improve quantum efficiency also increases the distance that the electron track must drift, thereby reducing the effective resolution, so that there is an optimum depth that maximizes the overall sensitivity.

The time-projection chamber (TPC) provides a means to overcome the diffusion limit with an alternate detector geometry[4,5]. This geometry decouples the electron diffusion from the quantum efficiency by having the electrons drift perpendicular to the X-ray propagation direction (Figure 1.1, right).

The TPC polarimeter uses a time-projection readout technique that forms pixel images of photoelectron tracks from a one-dimensional strip readout as illustrated in Figure 1.2. A micropattern proportional counter is read out with strip anodes oriented parallel to the propagation direction of the incident X-rays. Each strip is instrumented with a charge-sensitive amplifier and a continuously sampling analog-to-digital converter (ADC). The cathode is instrumented to provide a data acquisition trigger. A voltage applied between the drift electrode and the cathode establishes a uniform electric field in the active volume.

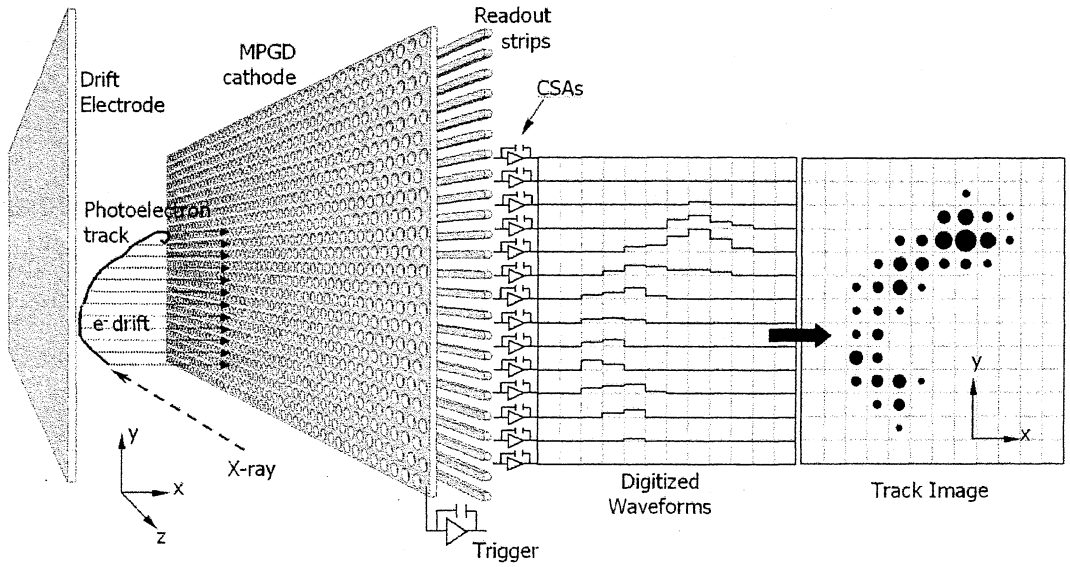

Figure 1.2 Left: The TPC polarimeter uses a simple strip readout and time of arrival to form a pixelized image of photoelectron track. Middle: The TPC polarimeter forms an image by digitizing the signal on each readout strip. The signal from a 6 keV X-ray, proportional to the charge pulse-train deposited on each strip, is shown on the right. The resulting image shows the interaction point, emission angle and end of the track. The size of each circle is proportional to the deposited charge in each virtual pixel; the grid is on a 132 μm spacing.

In a TPC polarimeter, the photoelectron is ejected preferentially in a plane parallel to the drift field. The ionization electrons then drift with a constant velocity to the cathode, where the charge is multiplied and collected on the strips. The active depth can be increased indefinitely without increasing the drift distance, at least to the extent that the X-ray beam is collimated.

Figure 1.2 illustrates how a track image projected onto the x-y plane is formed by digitizing the charge pulse waveforms and binning into pixels. The coordinates are defined by strip location in one dimension, and arrival time multiplied by the drift velocity in the orthogonal dimension.

The advantages of polarimetry techniques using micropattern gas detectors are:

- Analysis of the tracks enables reliable identification and rejection of charged particles and background events.
- The photoelectron emission angle can be reconstructed without *a priori* knowledge of the interaction point. Therefore, it is less susceptible to false modulations arising from asymmetries around the line of sight.

- This type of polarimeter has a broadband spectral capability of a proportional counter and can, in principal, be optimized to provide a sensitive bandwidth between 2 and 100 keV depending on the selected gas and pressure.

The TPC polarimeter has the following advantages that also make it an ideal detector for measuring the polarization of GRB prompt emission:

- It has a simple and inexpensive readout scheme that is attractive for large volume detectors.
- It has the capability for much larger quantum efficiencies and therefore, greater polarization sensitivity.

In the following sections, we will describe the TPC polarimeter concept in more detail and present results from a simple prototype device. We describe a Gamma-ray Burst Polarimeter (GRBP) for a mission of opportunity with the U.S. Naval Academy; MidSTAR-2, and a Low Energy Polarimeter (LEP) for a SMEX mission concept for a broadband polarimetry observatory; POET (POlarimeters for Energetic Transients).

2. TECHNICAL APPROACH AND METHODOLOGY

2.1 Detector Design and Readout Electronics

We have demonstrated the TPC polarimeter concept with a prototype instrument constructed from readily available, off-the-shelf components. The instrument consists of a micropattern proportional counter, strip readout, and encoding electronics.

The micropattern proportional counter is assembled from two etched stainless steel meshes, that form the cathode and anode, separated by an insulating spacer Figure 2.1 (centre). The dimensions of the stainless steel meshes are 50 μm thick with 75 μm diameter holes on 150 μm hexagonal spacing[4,5]. The meshes are mounted on frames under tension with their holes aligned and separated by a 100 μm thick Teflon spacer. The active volume is defined by an opening in the spacer (30 mm x 12.7 mm) and the drift electrode 2 cm above the cathode.

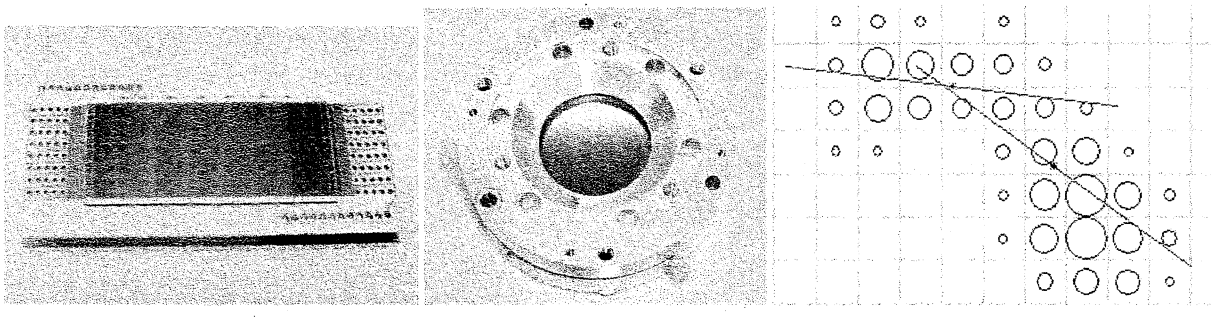

Figure 2.1 Left: Readout strips. Centre: The multiplication stage of a micropattern proportional counter. Right: A reconstructed track from a 6 keV X-ray interaction in Ne:DME. The red line shows the emission angle derived from a one-stage algorithm using the entire track. The green-upper line represents the angle derived from a two-stage algorithm and is significantly more accurate; the grid is on a 132 μm spacing.

The readout strips (Figure 2.1, left) are mounted 500 μm behind the meshes. The strips are on a pitch of 132 μm and are aligned with the mesh holes along one of the 60° symmetry axes of the meshes. The readout plane is a standard printed circuit board with 96 readout strips that are grouped into four sets of 24, by connecting together every 24th strip. Providing that an electron track crosses fewer than 24 strips, the track can be unambiguously reconstructed. This scheme can be expanded indefinitely in both length (detector depth) and width (number of sets of strips).

Each channel of readout electronics consists of a charge sensitive preamplifier, a low-noise fixed gain amplifier, a variable gain amplifier and an ADC. Each ADC is read out with a field-programmable gate array (FPGA) and the data are transferred to a host PC for event processing. When triggered, the system stores 512 ADC samples from each of 24 channels, 256 before the trigger, and 256 after the trigger. The system trigger is taken from the cathode signal using a zero-crossing timing discriminator.

The response of the TPC polarimeter has been measured in several gas mixtures; e.g. 50% neon, 50% dimethyl ether (DME) at 460 Torr[4,5] and in 83% neon 8% carbon dioxide and 8% carbon disulfide at 480 Torr. The prototype did not have an independent means of verifying the drift velocity, so unpolarized 5.9 keV X-rays from an ^{55}Fe source were used

to make adjustments to the drift field at the few percent level. With an incorrect drift velocity, the track images would be distorted such that a false modulation will occur at either 0 or 90 degrees. Histograms of the photoelectron emission angles of unpolarized X-rays were fit to the functional form $\alpha cos^2\phi + \beta sin^2\phi$ and the voltage on the drift electrode was adjusted to equalize the parameters α and β to give the expected uniform distribution. This technique will only work to the extent that other sources of asymmetry are negligible, which can be confirmed by an equal response to polarized X-rays at 0 and 90 degrees. Polarized 6.4 keV X-rays were produced by Bragg scattering iron K_α X-rays through 90 degrees off a silicon crystal. The X-ray beam was collimated and entered the active volume in a direction parallel to the readout strips at a height of 4 mm above the multiplication stage. The TPC was mounted on a stage so that it could be rotated around the axis of the X-ray beam. Data were taken with the phase of polarization oriented at 0, 45, and 90 degrees with respect to the electron drift direction. Unpolarized data were collected both before and after the polarized data to verify that there was no change in drift velocity during the measurements.

3. ANALYSIS

The data were analyzed by reconstructing the emission angle of each photoelectron from the direction of the major axis of the second moment of the charge distribution about its barycenter. To increase the polarization sensitivity, the analysis is performed a second time using only the information near the X-ray interaction point, where the angular information has been least affected by scattering[27]. The interaction point can be determined if the charge from the photoelectron and the Auger electron can be distinguished. This is possible by comparing the density of charge on one side of the barycenter to the other, where the higher density side is indicative of the Bragg peak, i.e. the end of the track. See Figure 2.1 (right). Histograms of the emission angles were then fitted to the expected functional form:

$$N(\phi) = A + B\cos^2(\phi - \phi_o) \qquad [1]$$

Where ϕ_0 is the angle of the plane of polarization. The response to 100% polarized X-rays defines the modulation factor, μ, given by:

$$\mu = \frac{N_{\max} - N_{\min}}{N_{\max} + N_{\min}} = \frac{B}{2A + B} \qquad [2]$$

Where N_{max} and N_{min} are the maximum and minimum of the function, respectively.

Because the measured modulation can never be negative, even an unpolarized source can give an apparent positive polarization. The sensitivity of a polarimeter is therefore expressed as the ***Minimum Detectable Polarization*** (MDP), i.e., the apparent polarization arising from statistical fluctuations in unpolarized data. The MDP is a function of instrumental properties as well as the source strength, S *(cts* $cm^{-2}s^{-1}$*)*, and the observing time, t. At the 99% confidence level:

$$MDP = \frac{4.29}{\varepsilon\mu SA}\left(\frac{\varepsilon SA + B}{t}\right)^{1/2} \qquad [3]$$

Where ε is the quantum efficiency, A is the collecting area, and B is the total background rate. However, the ultimate sensitivity may not be limited by statistics but by systematic errors created by false modulations that arise from azimuthal asymmetries in the instrument.

4. RESULTS

The results for Ne:CO_2:CS_2, shown in Figure 4.1 demonstrates the uniform sensitivity of the TPC polarimeter with respect to polarization angle. Fitting the expected functional form to the data (equation [1]), shows consistent modulations for all three angles with an average modulation factor of 42.4 ± 1.6 % at 6.4 keV and no false modulation at the one percent level, 0.1 ± 1.3 %, in the unpolarized case, see Table 4.1. Similar results are obtained for Ne:DME[4,5].

Table 4.1 Fit results to the reconstructed emission angles with reduced chi squared values. The errors stated are one standard deviation.

Data	Modulation	Error	Phase	Error
Unpol	0.1 %	1.3 %	-	-
0	39.6 %	2.7 %	2.5°	1.7°
45	43.3 %	2.7 %	41.3°	1.7°
90	44.4 %	2.8 %	89.2°	1.5°

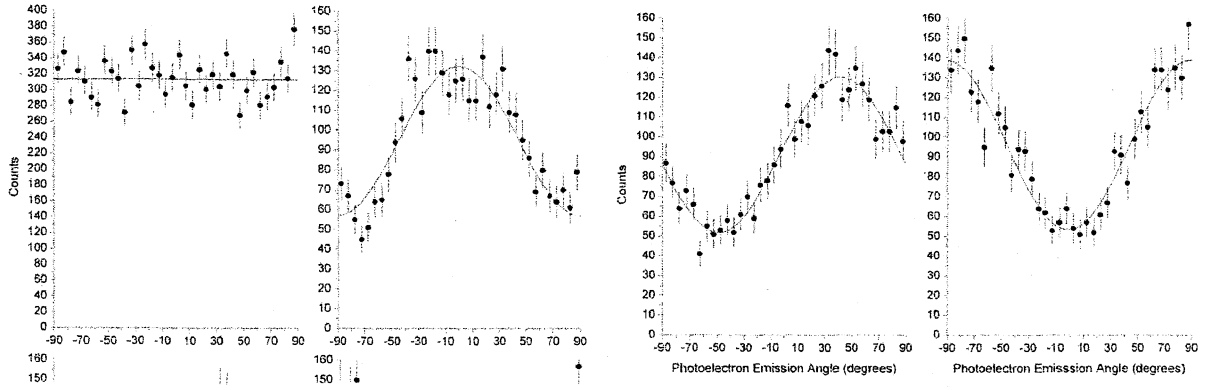

Figure 4.1 Results for Ne:CO_2:CS_2 at 480 Torr . Histograms of photoelectron emission angles for a 6 keV unpolarized source, 6.4 keV polarized X-rays with phases of 0°, 45° and 90° with respect to the drift direction from left to right, respectively. The modulations and phase are given in Table 4.1.

5. GRB POLARIMETRY MISSION CONCEPTS

5.1 GRB X-ray Polarimeter Requirements

The limited duration and isotropic distribution of GRBs, requires a polarimeter with a large field of view and high sensitivity. A time-projection chamber (TPC) polarimeter is the ideal solution. It provides high quantum efficiency, low mass and power with unmatched polarization sensitivity over the 2-10 keV band-pass and expected up to 50 keV. To optimize the detector for GRB polarimetry, the concept uses a negative ion drift gas[20,21,26] in combination with a large area micropattern proportional counter. Because the GRB prompt emission is exceptionally bright and expected to be highly polarized, successful measurements can be made even with a small instrument. The duration of the prompt emission from the GRB itself spans several orders of magnitude from 0.01 seconds to more than 1000 seconds, with typical durations of about 20 seconds for a long burst. This allows pre- and post- burst background measurements that can be used to minimise systematic effects arising from background variations. The burst flux exhibits rapid time variability, however it only needs to be resolved at the ~1 second level for polarimetry measurements in order to determine the duration over which the fluence is released. Therefore, the electronics are only required to be fast enough to avoid pile-up in the detector, thus reducing the power, although the ability to measure rapid time variability is advantageous especially for other bright periodic sources.

5.2 Detector Design: Negative Ion Drift TPC Polarimeter

Several parameters can be optimized to maximize the sensitivity of a TPC polarimeter in the required energy band; the gas composition and pressure, the geometric area of electron multiplication stage, the distance between drift electrode and the multiplication stage, and the spacing of the readout electrodes (pitch).

Selecting a gas requires consideration of the drift speed, diffusion rate and mean atomic number:

- A gas with low drift velocity is desirable to achieve high photoelectron spatial resolution with low-speed and low-power electronics, as high time resolution (< 1ms) is not required for GRB polarimetry.

- A gas with a low electron diffusion rate allows a larger drift distance before the photoelectron track is lost in the diffused charge cloud. This enables detectors with larger effective areas.
- Increasing atomic number increases stopping power and therefore increases the quantum efficiency of a detector for a given size and gas pressure. But increasing Z also increases the number of elastic scatters compared to inelastic scatters, making it harder to reconstruct the initial direction of the photoelectron.
- The highest modulation is produced when the incident X-ray energy is more than twice the K-shell energy of the absorber.

For a 2-10 keV polarimeter, a negative-ion drift TPC, using carbon disulfide (CS_2) as the charge-carrying ion in neon, is an attractive concept because of its extremely low diffusion[20,21,26] and slow drift speed allowing the photoelectron track to be read out by much slower electronics (factor of ~100 compared to Ne:DME), which require much less power. The fact that CS_2 has a very low diffusion rate means that the drift-multiplication stage separation can be quite large without the diffusion of the charge cloud degrading the track information. This enables larger effective areas for a single detector. In addition, the timing calibration of a slower moving charge cloud is likely to be more stable and less susceptible to small changes in the environment. A small quantity of CO_2 is added to the gas mixture as a quench gas. We have characterized the prototype detector in Ne:CO_2:CS_2 to determine the minimal partial pressure of CS_2 (~40 Torr) for optimal drift speed and minimal diffusion. Laboratory tests using Ne:CO_2:CS_2 at 480 Torr with 132 μm readout strips produce modulation curves as shown in Figure 4.1. For a higher energy polarimeter, 15-50 keV, an argon based gas mixture, rather than neon, is more appropriate.

5.3 The MidSTAR-2 Mission of Opportunity

The United States Naval Academy (USNA) Small Satellite Program provides the opportunity to train USNA Midshipmen majoring in Aerospace Engineering with hands on satellite development and operations experience. The Midshipman Space Technology Applications Research (MidSTAR) project allows them to work on a platform for small payloads that can be rapidly adapted to a variety of applications and missions at relatively low cost. MidSTAR-1 was successfully launched on 8 March 2007 with five small payloads from the USNA, the Naval Postgraduate School and NASA.

MidSTAR-2 will use the same basic architecture as MidSTAR-1 with increased performance in one or more areas such as power, attitude control, and telemetry bandwidth. The MidSTAR-2 spacecraft is being designed to accommodate four small payloads from the Goddard Space Flight Center, one of which is the Gamma-ray Burst Polarimeter (GRBP). Each payload will be designed to require less than 6 Watts orbit averaged power, weigh less than 6 lbs and occupy a volume less than 23 x 27 x 8 cm^3.

Table 5.1 GRBP baseline properties

Mass	< 2.7 kg
Active Volume	12 x 12 x 5 cm^3
Power (oper/ave)	8 W / 6 W
Data vol/burst	100 Mbyte
Field of view	1.0 steradian
Operating Temp	-10 to 25° C
Active Element	Ne:CO_2:CS_2 650:80:40
Pressure	>760 Torr
Max. drift distance	3 cm
Readout pitch	75 μm
Peak Sensitivity	~3.5 keV

Figure 5.1. The preliminary GRBP instrument configuration on MidSTAR-2

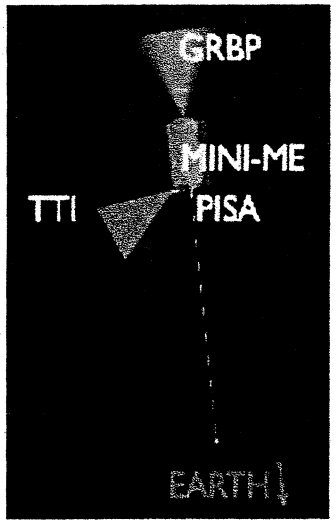

MidSTAR-2 will be launched from the Evolved Expendable Launch Vehicle (EELV) Secondary Payload Adapter (ESPA) ring that allows up to six small secondary payloads (SPL) as a ride-along on the EELV. MidSTAR-2 is a Class D platform, which will use commercial off-the-shelf components to minimize cost and for rapid turn-around. The spacecraft will be an octagonal prism approximately 1 m in length and less than 40 cm in diameter. The current design is a gravity gradient stabilized platform with a slow spin (baseline 13 min/revolution) about the boom axis. The GRBP will be a zenith pointing experiment capable of long exposures to the sky as required by a gamma-ray burst monitor, see Figure 5.1. MidSTAR-2 has a possible launch date in mid-2011.

5.4 MidSTAR-2 Gamma-Ray Burst Polarimeter (GRBP) design

Mechanical: The approach is to build a modular instrument based on the prototype TPC polarimeter. The instrument will consist of four detector units with a total active geometric area of 12 x 12 cm^2. Each detector unit (6 x 6 cm^2) will have two TPCs that share an X-ray transparent drift electrode (see Figure 5.2, left). A single gas volume and X-ray window is shared by two detector units. Table 5.1 summarizes the instrument properties.

The GRBP housing envelope available on the interior of MidSTAR-2 (8 cm) limits the detector depth to 5 cm in order to have sufficient space to bring the signals out. The 3 cm maximum drift distance ensures that the track images will not be degraded by electron diffusion as the ionization electrons drift toward the multiplication and readout stages. In order to create a uniform electric field (~1% in magnitude and a few degrees in direction) between the drift and the multiplication stage, field-shaping electrodes will surround each active volume.

A 5 cm tall collimator or baffle (limited by the MidSTAR-2 envelope) will be installed in front of the window to limit the field of view of the detector to background X-rays to 1 steradian and to protect the window from micrometeoroids.

Electronics: The readout plane is 5 x 6 cm^2, with strip electrodes 5 cm long on a 75 μm pitch to optimize the track sampling for an operational pressure of ~770 Torr. In each detector unit, every 24th strip will be tied together. The four units require a total of 96 signal-processing chains. To minimize noise, each signal will be pre-amplified by a source-follower inside the gas volume. The signals will feed-through to the exterior electronics box, where each signal will be amplified by a low-power op-amp at the input to an ADC. This enables much more efficient power dissipation preventing the detector environment from being perturbed by the heat dissipated by the electronics.

For the expected drift field, the electron drift velocity is ~40 ms^{-1}. In order to resolve 75 μm pixels in the time dimension an ADC with ~500 kHz sampling will be required. The power goal is <10 mW/channel; pre-amp, ADC driver and ADC. We have identified the SIDECAR ASIC[18] as an available, low power candidate suitable for this application. We will use a Field-Programmable-Gate-Array (FPGA) (similar to the design currently used in-house to drive the prototype) to drive the ADC readouts, to perform event analysis and to package the telemetry.

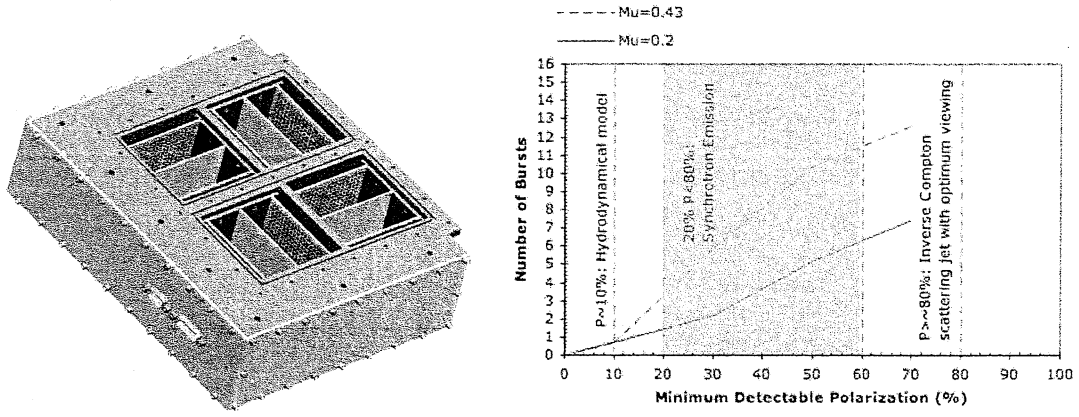

Figure 5.2 Left: The GRBP instrument housing solid model (with the FoV baffle and window removed) containing four 6 x 6 x 5 cm^3 detector units. Two detector units occupy a single gas enclosure. The electronics will be mounted in the remaining volume outside of the gas volume. Right: Polarization Sensitivity of the GRBP (assuming 80% duty cycle) for two modulations factors; 0.43 (dashed) as measured at 6.4 keV and 0.2 (solid) the lower bound expected at 2 keV.

Two controllable high voltage supplies will be used: A negative supply for the drift electrode to allow adjustment of the drift velocity and a positive supply to control the anode and the strips relative to the grounded cathode to adjust the gain. The negative supply will also provide the voltages for the field cage around each detector.

Data Processing and Operations: For every event that triggers the GEM cathode, the flight software will read the 24 x 24 array of pixels from the ADCs and push the data into a FIFO buffer. The buffer will be sized to hold ~15 minutes of background and the events from the brightest, longest duration burst. As new data are pushed into the buffer, old data will be pushed out and nominally discarded until the software detects a burst. During non-burst periods, a background event will be telemetered to the spacecraft. These background events will be used on the ground for drift speed calibration and to define the sensitivity.

The software will be monitoring the background countrate. When the countrate increases to a designated value above the background, the software will switch into a burst mode. Data stored in the buffer from the prior ~5 minutes will be stored and a further ~10 minutes of data (depending on the brightness of the burst) will be pushed into the buffer. The flight software will process the events to produce quick-look (QL) lightcurves and time-stamped reconstructed emission angles. These data will be telemetered to the spacecraft first to ensure that the high priority data are downlinked to the ground successfully. Following the QL data and prior to the next burst, the 24 x 24 event data will be telemetered, to allow post-processing and optimization of thresholds on the ground.

5.5 GRBP Polarization Sensitivity

To understand the GRBP configuration that will achieve the lowest possible minimum detectable polarization for GRBs in the 2-10 keV energy band, and to optimize the instrument concept with regard to gas composition, pressure, window thickness and drift distance, we selected GRBs from the HETE-2 catalog from the beginning of the mission to 13 September 2003 which were detected both in the wide-field X-ray monitor (WXM; 2-25 keV) and the French Gamma telescope (FREGATE; 6-400 keV). 45 bursts satisfied these criteria[31,32]. The fluence in the 2-10 keV energy band was determined from a spectral fit to the data from each burst and a table of T_{100} (the duration for 100% of the flux to be emitted) and average flux over the T_{100} duration was created.

Using a power-law spectrum (valid for energies below E_{peak}) of photon index 1, the photon spectrum over the 2-10 keV energy band was derived for a flux of 1×10^{-8} erg cm^{-2} s^{-1}. The instrument response to the photon spectrum, for the instrument parameters in Table 5.1, was calculated and then scaled for the flux and T_{100} for each of the 45 HETE-2 bursts. The Instrument response to a background spectrum9 was also calculated over the T_{100} duration.

The MDP for each of the 45 bursts was calculated using two modulations factors; the first, 0.43, is the measured value from the prototype TPC at 6.4 keV, the second value of 0.2, is to bound the sensitivity as a lower modulation factor is expected at lower energies27. Accounting for the HETE-2 FoV (0.9 str) and the time period over which the catalog was obtained (~ 3 years operational time including periods in the SAA), and scaling the distribution of bursts to the GRBP field of view, the number of bursts for a given MDP was determined for the mission life-time. Figure 5.2 (right) shows the expected number of bursts that will be detected if the polarization is above the sensitivity limit (MDP). To show the significance of the measurements the expected GRB polarization for several of the leading models is shown. The maximum observable polarization expected for synchrotron emission is 60%[12,13,19] whereas for inverse Compton models, the maximum polarization can be as high as 100% for a narrow jet with optimum viewing angle[8,16]. This clearly demonstrates that the GRBP will be able to make ground-breaking measurements, distinguishing between models. The GRBP will measure the polarization of 10 GRBs with an MDP of 10-50%.

5.6 POlarimeters for Energetic Transients (POET)

POET (POlarimeters for Energetic Transients) is a small explorer (SMEX) concept for a broadband polarimetry observatory and consists of two types of polarimeter. A high energy Compton scattering polarimeter, GRAPE (Gamma-RAy Polarimetry Experiment[17,22]) with a bandpass of 50-500 keV and two photoelectric time-projection chamber polarimeters optimized for two energy ranges; 2-10 keV and 15-50 keV. The concept for the instrument configuration on the optical bench is shown in Figure 5.3.

POET will explore many areas of X-ray and gamma-ray polarimetry; e.g. GRBs, solar flares, SGRs, bright persistent sources, phase resolved polarimetry of bright transient sources and, in addition, will provide broadband (2-500 keV) all-sky monitoring. For this paper, we focus on the GRB polarization sensitivity. POET, with its high timing resolution (msec) and broadband spectral capabilities will provide information about the prompt GRB emission that cannot be obtained from current prompt and afterglow observation strategies without polarization measurements:

- The composition of GRBs (baryonic or Poynting-flux dominated).
- The radiation mechanism of the prompt gamma-ray emission (synchrotron or inverse Compton).
- The small-scale geometry of the prompt emission region.

These questions could be answered with a good sample of polarization measurements of GRB prompt emission from a mission such as POET.

GRAPE: The GRAPE concept and design has been described in detail elsewhere[17,22]. The baseline design for the POET GRAPE instrument is an 8 x 8 array of GRAPE modules using NaI scintillators as calorimeters and plastic scintillator as the scattering medium. The separate readout design places all the plastic elements on two-inch flat-panel photomultiplier tubes, with separate readouts of calorimeter elements, to avoid cross-talk between adjacent scatterer and calorimeter elements. The GRAPE configuration for the POET mission is given in Table 5.2 and the resulting GRB sensitivities are shown in Table 5.2 and Figure 5.3. Figure 5.3 shows the number of bursts of a given fluence from the BATSE catalogue that will be detected by GRAPE versus the limit in polarization sensitivity for those bursts, i.e. the minimum detectable polarization (MDP). If the burst polarization is greater than the MDP then GRAPE will provide a definitive polarization measurement, if the polarization is below the MDP then only an upper limit will be obtained. If the polarizations of the detected GRBs are greater than 30%, GRAPE will measure the polarization of 50 bursts in a year. If the GRB polarizations are as low as 10% then GRAPE will measure the polarization of 14 bursts/year.

Low Energy Polarimeter (LEP): The LEP design and operational concept is based on the design described for the GRBP on the MidSTAR-2 mission (Section 5.4). The larger spacecraft available for a SMEX mission yields higher mass and power allocations and thus enables an instrument with larger volume and is therefore more sensitive. For POET, the two 2-10 keV LEP modules will have orthogonal 1-D coded-masks aligned with the strip readout in order to provide course position information (~3 degrees). This will be used to correct the polarization angle for off-axis GRBs. The LEP design parameters for the 2-10 keV and the 15-50 keV instruments are given in Table 5.2 and the resulting sensitivity to GRBs is shown in Table 5.2 and Figure 5.3. Figure 5.3 shows the number of bursts from the HETE-2 catalogue of a given fluence that will be detected by the two LEP instruments versus the limit in polarization sensitivity for those bursts (the analysis is described in more detail in Section 5.5). If the burst polarization is greater than the MDP then LEP will provide a definitive polarization measurement, if it below then only an upper limit will be obtained. In a year, if the detected GRBs are polarized more than 30% then the 2-10 keV LEP will measure the polarization of more than 35 bursts. If the GRB polarization is as low as 10% then the 2-10 keV LEP will measure the polarization of 17 bursts.

Table 5.2 Preliminary instrument design and sensitivity summary for POET

	Low Energy LEP	**High Energy LEP**	**GRAPE**
Energy Range	2-10 keV	15-50 keV	50-500 keV
Active Area	35x35 cm^2	35x35 cm^2	64 x 64 cm^2
Active Depth	30 cm	30 cm	5 cm
FoV	1 str Coded Ap.	1 str	$>\pi$ str
Active material	Ne:CO_2:CS_2	Ar: CO_2:CS_2	LaBr3/CsI
Window	Be or Mylar	Be or Mylar	N/A
Pressure	1.1 atm	3 atm	N/A
# Burst/yr MDP<30%	>35	20	50
# Bursts/yr MDP<10%	17	6	14

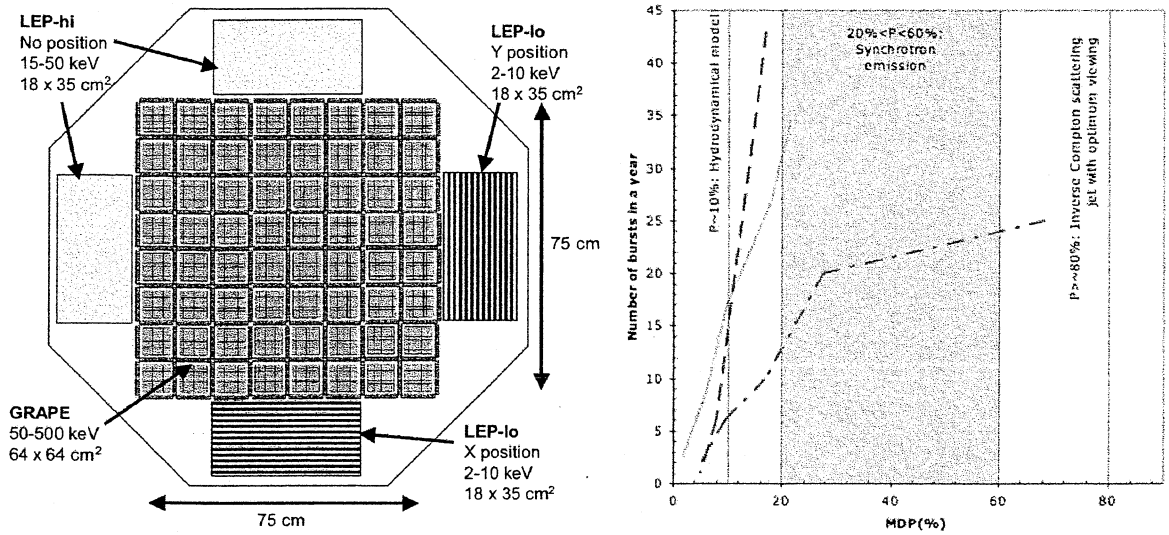

Figure 5.3 Left: The instrument layout on the POET optical bench. Right: The number of bursts expected to be detected for a given sensitivity (MDP) for GRAPE (dashed) and the high (dot-dash) and low (solid) energy LEP. To show the significance of the measurements the expected GRB polarization for several of the leading models is shown.

6. CONCLUSION

An instrument designed to make measurements of the polarization of the prompt GRB emission would provide a qualitative and quantitative leap forward in our understanding of the mechanisms driving GRB explosions and lay the path for future X-ray polarimetry measurements.

We have demonstrated that the time-projection chamber polarimeter is ideally suited to wide field of view, large area applications for the 2-10 keV bandpass and that its operation can , in principal, be extended up to 50 keV by selection of the appropriate gas and pressure. The GRBP, a small instrument with an active area of 24 x 24 cm^2 and an active depth of 6 cm, will measure 10 bursts with a sensitivity limit of 10 - 50% over the 2-10 keV bandpass during the two years of operation of MidSTAR-2.

POET, is a larger mission concept for a small explorer, will provide highly sensitive broadband polarimetry with simultaneous spectroscopy and photometry, by the use of a high energy Compton scattering polarimeter (GRAPE; 50-500 keV) and two types of Low Energy Polarimeter (LEP) optimized for 2-10 keV and 15-50 keV. This mission would measure the polarization of 40-50 GRBs per year with a sensitivity limit of 30% and 15-20 GRBs with a sensitivity limit of 10%. We are investigating the possibility for telemetering rapid positions to the ground in order to obtain the red-shifts from ground based follow-up which would provide additional constraints on the GRB models.

In addition to polarization measurements of GRB prompt emission and other bright X-ray transients and persistent sources, both missions would demonstrate the TPC polarimeter capabilities in preparation for larger future missions: e.g. Constellation-X enhancement package for faint for persistent sources[14] or wide field of view instruments for EXIST.

REFERENCES

1. Bellazzini, R. et al., 2004, *Nucl. Instr. Meth. A.*, **535**, 477
2. Bellazzini, R. et al., 2006, *Nucl. Instr. Meth. A,* **566** 552
3. Black, J.K. et al., 2003, *Nucl. Instr. Meth. A.* **513**, 639
4. Black, J.K. 2007a, *J. of Physics conference series*, **65**, 012005
5. Black, J.K. et al., 2007b, submitted to *Nucl. Instr. Meth. A.*,

6. Coburn, W. and Boggs, S.E. 2003, *Nature*, 423, 415

7. Costa, E. et al., 2001, *Nature*, 411, 662

8. Dar and De Rujula, 2004, *Physics Reports*, **405**, 203

9. Dean, A.J., et al. 2003, *Space Sci. Rev.*, **105**, 285

10. Fan, Y.Z., Zhang, B., & Proga, 2005, D. *ApJ*, **635**, L129

11. Gehrels, N., et al. 2005, *Nature*, **437**, 851

12. Ghisellini, G. and Lazzati, D. 1999, *MNRAS,* **309**, 7

13. Granot, J. 2003, *ApJ.*, **596**, 17

14. Jahoda, K., et al., *eprint arXiv*:astro-ph/0701090

15. Kalemci, E., et al., 2007, *ApJS*, **169**, 75

16. Lazzati et al. 2004, *MNRAS*, **347**, 1

17. Legere, J., et al., 2005, *Proc. SPIE*, **5898**, 413

18. Loose, M., et al. 2006, *Proc SPIE*, **6265**, 62652J-1

19. Lyutikov, M. et al. 2003, *ApJ.*, **597**, 998

20. Martoff, C. J., et al. 2000, *Nucl. Instr. Meth, A.*, **440**, 355

21. Martoff, C.J., et al., 2005, *Nucl. Instr. and Meth. A.*, **555**, 55.

22. McConnell, M. L., et al. 2004, *Proc. SPIE*, **5165**, 334

23. McGlynn, S., et al., 2007, *A&A*, **466**, 895

24. Novick, R., et al. 1972, *ApJ*, **174**, L1

25. Novick, R., 1972, in: T. Gehrels (ed.), *Planets, Stars and Nebulae Studied with Photopolarimetry*, University of Arizona Press, 262

26. Ohnuki, T., Snowden-Ifft, D.P., & Martoff, C.J. 2001, *Nucl. Instr. Meth. A.*, **463**, 142

27. Pacciani, L. et al., 2003, *Proc SPIE*, 4843, 394

28. Paczynski, B. 1998, *ApJ*, 494, L45

29. Rees, M.J. & Meszaros, P. 1994, *ApJ*, 430, L93

30. Rutledge R.E. and Fox D.B., 2004, *MNRAS*, 350, 1288

31. Sakamoto, T., 2004, "Spectral characteristics of X-ray flashes and X-ray rich gamma-ray bursts observed by HETE-2", *Thesis*

32. Sakamoto, T., et al, 2005, *ApJ.*, **629**, 311

33. Sauli, F. 2004, *Nucl. Instr. Meth. A.*, **522**, 93

34. Weisskopf M.C., et al., 1978, *ApJ.*, **220**, L117

35. Wigger, C. et al. 2004, *ApJ*, **613**, 1088

36. Willis, D.R., et al., 2005, *A&A*, **439**, 245

37. Zhang and Meszaros, 2004, *International Journal of Physics A*, **19**, 2385